REAL TIME PREDICTIONS OF THREE NUMERICAL MODELS OF THE ARRIVAL AT THE EARTH OF ELEVEN FLARE/HALO CME ASSOCIATED SHOCKS COMPARED WITH SPACECRAFT MEASUREMENTS

S.M.P. McKenna-Lawlor[(1)], M.Dryer[(2,3)], Z. Smith[(3)], K. Kecskemety[(4)], C.D. Fry[(2)],W. Sun[(5)], C.S. Deehr[(5)], D. Berdichevsky[(6,7)],K.Kudela[(8)] and G. Zastenker[(9)].

[(1)] Space Technology Ireland, National University of Ireland, Maynooth, Co. Kildare, Ireland.
[(2)]Exploration Physics International, Inc., Milford, New Hampshire, 03055, USA.
[(3)]NOAA Space Environment Center, Boulder, Colorado, 80305, USA.
[(4)]KFKI Research Institute for Particle and Nuclear Physics, Budapest, Hungary.
[(5)]Geophysical Institute, University of Alaska, Fairbanks, Alaska, 99775, USA
[(6)]Emergent Information Technologies, Inc., Largo, Maryland, 20774, USA.
[(7)]Laboratory for Extraterrestrial Physics, NASA, GSFC, Code 690, Greenbelt, Maryland, 20771, USA.
[(8)]Institute for Experimental Physics, Kosice, Slovakia.
[(9)]Space Research Institute, Moscow, 117997, Russia.

ABSTRACT

Three widely used numerical models, namely the Shock Time of Arrival Model (STOA); the Interplanetary Shock Propagation (ISPM) Solar Wind Model and the Hakamada-Akasofu-Fry (HAFv.2) model were used to predict the times of arrival at the Earth of 11 Flare/Halo CME associated shocks. These predictions were then compared with measurements made aboard various near-Earth spacecraft (at or within ~ 300 R_E of Earth) in plasma, magnetic field and energetic particle data. STOA provided the smallest values of the (predicted minus observed) arrival times and showed a typical precision better than about 8h. The ratio of the error estimate for each model to the standard deviations of the observations was 0.56, 1.2 and 1.0 for STOA, ISPM and HAFv.2 respectively for the small number of events considered. Larger statistical samples should now be tested. HAFv.2 provides special insights into the conditions under which individual shocks propagate. Ways to improve the performance of the models tested are suggested.

1. INTRODUCTION

Real time predictions of the arrival at the Earth of interplanetary shocks associated with eleven Flare/Halo CMEs were made using three widely used numerical models. The eleven solar events initiating these shocks, together with information concerning their associated metric Type II bursts, CME, X-ray radiation and disk locations are listed in Table 1 (for details see caption).

2. OVERVIEW OF THE NUMERICAL MODELS

The Shock Time of Arrival (STOA) Model, see for example [1], is based on the similarity theory of blast waves (modified by the piston driving concept) that emanate from point explosions. The initial explosion (flare) drives a shock at what is assumed to be a constant speed for a specified length of time ***(tau),*** estimated using X-ray measurements. Column 8, Table 1 provides such data from GOES-8 measurements for the 11 events considered here. Shock speed estimates provided by Type II burst radio observers at various sites (Column 9) and CME velocities determined by the Large Angle Spectroscopic Coronagraph (LASCO/SOHO) Team (Col. 10) are also displayed in the Table.

The Interplanetary Shock Propagation Model (ISPM) is based on a 2.5 D magneto-hydrodynamic parametric study of numerically simulated shocks which shows that the net energy input to the solar wind is the organizing parameter [2]. Both the STOA and ISPM models require the initial coronal shock velocity, the input energy duration and the location of the source on the Sun as input observational data. STOA also requires the 'Parker Type' solar wind velocity profile up to 1 AU (obtained from L1 measurements) while ISPM employs a fixed internal model with a representative speed of 360 km/s at 1 AU.

HAFv.2 kinetically projects the flow of the solar wind from inhomogeneous sources near the Sun out into interplanetary space and adjusts the flow for stream-stream interactions as faster streams overtake slower ones. Solar surface magnetograms are projected, via the assumption of potential theory, onto the source surface at R = 2.5 Rs to provide both radial magnetic field and solar wind speed, as in [3]. During solar flares, energy is deemed to be input at the inner computational boundary. Electromagnetic measurements provide information on the start time, disk location and evolution of the energy source. Disturbance energy is made manifest by enhanced solar wind speed at the source surface. The

resulting compression is represented by time-dependent stream boundaries. Stream-stream interactions may lead to the production of shocks.

Unlike STOA and ISPM, HAFv.2 models the inhomogeneous ambient solar wind that affects the propagation of disturbances *en route* from the Sun to the Earth. Realistic inner boundary conditions determine the modeled background IMF topology and solar wind flow. These data are derived from maps of the magnetic field and solar wind velocity and this information is available from the National Oceanographic and Atmospheric Administration/ Space Environment Center (NOAA/SEC) where it is updated once per day.

3. MODEL OUTPUTS

STOA and ISPM predict whether a shock will arrive at the Earth and, if so, when. Is this regard they each provide a measure of shock strength, expressed in the case of STOA by the shock magnetoacoustic Mach Number (Ma) and in the case of ISPM by the Shock Strength Index (SSI). HAFv.2 predicts the solar wind speed, density, dynamic pressure and the IMF vector as functions of time at any point in the heliosphere (for the present application at L1). The temporal, running stepwise, profile of the predicted dynamic pressure at L1 is used to compute a Shock Searching Index (SSI).

4. COMPARISON OF PREDICTED WITH MEASURED SHOCK ARRIVAL TIMES

In the jargon of predictive weather forecasting methodology adopted at NOAA/SEC, the results of comparing predicted with measured arrival times are graded by the terms; HIT (h), MISS (m), FALSE ALARM (fa) and CORRECT NULL (cn). These terms are used to draw up Contingency Tables to display how different models score for particular events, as in [4]. HITS, MISSES and CORRECT NULLS are defined below (no FALSE ALARM occurred in our sample).

- HIT; If a shock is predicted to arrive at the Earth within a period up to 100h after a particular solar event and if the shock concerned is actually detected within ± 24h of this predicted time, that prediction constitutes a HIT.
- MISS; When an interplanetary shock generated in association with flare activity arrives at the Earth within 100h of its detection at the Sun but was not predicted to arrive within ± 24h of this time, the event constitutes a MISS.
- CORRECT NULL; When an interplanetary shock is predicted to arrive at the Earth following a particular solar event and indeed up to 100h thereafter no shock attributable to that event arrives this is a CORRECT NULL.

The threshold values for predicting an event in the present study were chosen as follows.

- The Mach Number for STOA must be > 1.00
- The Shock Strength Index for ISPM must be > 0.0
- The Shock Searching Index for HAFv.2 must be > -0.5 and the dynamic pressure jump across the simulated shock must be > 8 nPa.

Table 2 (Cols. 2-4) provides the dates and times of arrival at Wind (W) and at ACE (A) of interplanetary shocks generated by the solar events described in Table 1. It is noted that, when two or more solar events are spatially and temporally close to each other their associated shocks can potentially interact [5]. There are two such closely spaced pairs (Events 4 and 5 and Events 9 and 10) in the present sample. These pairs are indicated by shading in Table 2. Columns 15-17 provide the delta values (predicted minus observed arrival time) for the individual models (STOA, ISPM, HAFv.2). Columns 18-20 of the Table indicate events that can resultingly be categorized as HITs (h), MISSs (m) and Correct Nulls (cn) according to the above definitions.

For the 11 events considered, the models attained a generally high level of success in predicting, based on real time data, shock arrival at L1. Predictions generated using the ISPM and HAFv.2 models only fell outside the threshold limit of 24h required to score a hit in the case of Event 1. *Ex post facto* analysis indicates, however, that shock speeds adopted by the forecasters in 1997 may not have been realistic. Overall, the data indicate that STOA scored the smallest values of 'predicted minus observed' arrival times (typical precision better than 8h). The ratio of the error estimate for each model to the standard deviations of the observations was 0,56 1.2 and 1.0 for STOA, ISPM and HAFv.2 respectively. Larger statistical samples should now be tested. Initial steps have been taken using 36 events comparing the performances of STOA, ISPM and HAFv.1 in terms of contingency tables and conventional skill scores commonly used in meterology [3 and 6].

5. SPECIAL INSIGHTS PROVIDED BY HAFV.2

HAFv.2 is particularly useful in that it provides, based on its solar input parameters, information on the non-

uniform conditions in the heliosphere through which shocks propagate, while also monitoring how the COBpoint (which influences particle rise times for temporal flux enhancements) changes with time. The model also simulates the development of shock deformations on a scale of fractions of an AU. Such deformations can result from the influence of upstream structural inhomogeneities. An influence may further be exerted due to variations in the spatial profile of the driver ejecta.

Fig.1 presents a set of HAFv.2 ecliptic plane simulations for 12 May 1997, individually separated in time by 12h. The IMF lines are shown out to 2 AU. Earth is represented by a large black dot, Venus and Mars by smaller black dots. Starting at 0000 UT, compressed regions of spiral IMF indicate that four CIRs, viewed from above the Sun's North Pole, were already established in the heliosphere. In subsequent frames, these CIRs are seen to rotate counter-clockwise. In Frame 4 a CIR overtakes the Earth (~ 1200 UT, 13 May). The near Earth interplanetary region was characterized at that time by being in a "toward" IMF sector, showing enhanced solar wind velocity, density and IMF magnitude. In this scene, the leading edge of the interplanetary shock has advanced to about 0.3 AU with the center of the shock envelope directed along the Sun-Earth line. In Frames 5 and 6 the shock continues to advance along a line directed towards the Earth. The Shock-Earth connected lines map to a longitude well to the west of the Central Meridian (CM). The temporally changing point of connection to the shock of these IMF lines is the COB (Connection with OBserver) point defined in [7]. In Frame 7 which corresponds to 15 May at 0000 UT, the simulated shock is seen to be just about to intersect with the Earth, thereby agreeing with experimental data recorded aboard SOHO and Wind which show that a shock occurred at L1 at ~ 0115 UT. The *ex post facto* prediction which is based on adopting a realistic value (Vsh = 500 km/s) for the shock velocity is a considerable improvement ΔTh = -1h on the 'real time' prediction ΔTh = -31h given in Table 2, Column 17, initially derived taking Vsh = 1400 km/s.

The Earth connected IMF lines are shown in Frame 7 to map back to the Sun at western longitudes that are much nearer to the Sun-Earth line than was the case in earlier frames. On 15 May at 1200 UT (last frame) the leading edge of the modeled shock has propagated beyond the Earth's orbit. Its envelope is distorted because the shock is seen to have advanced faster on its western flank (when compared with its motion along the CM line) as it rode over regions of higher speed ambient solar wind streams.

6. STEPS TO IMPROVE MODEL PERFORMANCE

- All the models showed extreme sensitivity to uncertainties in determining the initial coronal shock velocity. Development of a global 3D coronal density model, temporally and spatially appropriate for specific events is recommended to overcome this problem.
- For improved performance, HAFv.2 should be upgraded to a full 3D MHD model when the required codes mature to a point where they can be run in real time using the available observational data inputs.
- Uncertainties in the input data resulted in the setting by the forecasters of thresholds for detecting HITS and MISSES that allowed the shocks associated with those large, Earth directed, halo CMEs studied here to be successfully predicted. Events of lower energy could have, in general, been missed. Statistical studies of relatively large samples are now required to provide guidance as to the criteria to be adopted when modeling the propagation of weaker shocks through the generally non-uniform interplanetary medium.

REFERENCES

1. Dryer, M. Interplanetary shock waves generated by solar flares, *Space Sci. Rev*., **15**, 403-468,1974.
2. Smith, Z. and Dryer, M. MHD study of temporal and spatial evolution of simulated interplanetary shocks in the ecliptic plane within 1 AU, *Solar Phys.* **129**, 387-405, 1990.
3. Fry, C.D. et al. Improvements to the HAF solar wind model for space weather predictions, *J. Geophys. Res*., **106**, 20,985-21,001, 2001.
4. Schaefer, J. T., Critical success index as an indication of warning skill, *Weather Forecasting*, **3**, 570-575, 1990.
5. Smith,Z.K. et al. Interplanetary shock collisions: forward with reverse shocks, *Astrophys. Space Sci*., **119**, 337-344, 1986.
6. Smith et al. Performance of interplanetary shock prediction models *J. Atm. Terr. Phys.* **62**,1265-1274,2000.
7. Lario et al. Energetic particle events: Efficiency of interplanetary shocks as 50 keV < E < 100 MeV proton accelerators *Astrophys. J.* **509**, 415-434, 1998.

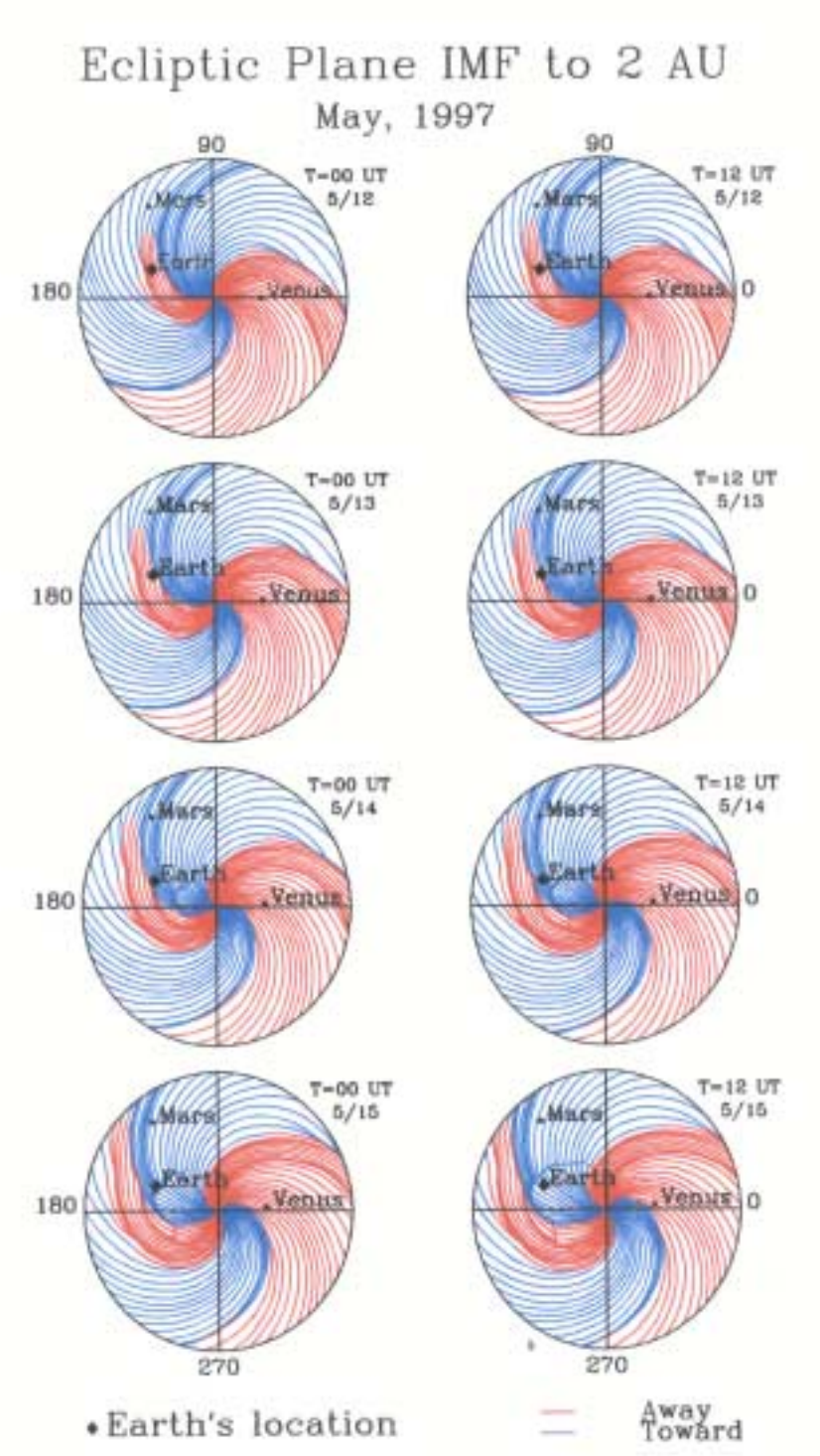

Figure 1. Ecliptic plane simulations by the HAFv.2 model of the temporal IMF disturbance caused by the shock from Event 1 that was initiated on 12 May 1997. Polarity is indicated by blue (toward the Sun) and by red (away). The location of the Earth is indicated by a large black dot; of Venus and Mars by smaller dots.

Table 1: Characteristics of Eleven Solar Flares with accompanying Metric Type IIs and Halo CMEs.

1	2	3	4	5	6	7	8	9	10	11
Event No.	Date **YYMMDD**	**Start (UT) II**	**CME**	**Max.(UT) X-ray**	**Flare class**	**Flare Location**	**tau** (h)	**Vs(II)** (km/s)	$\mathbf{V_{cme}}$ (km/s)	$\mathbf{T_{cme}-T_{II}}$ (h:m)
1	19970512	0516	0630	0516	C1/1F	N21 W08	2.50	1400	306	1:14
2	19971104	0608	0610	0554	X2/2B	S14 W33	1.25	1400	830	0:02
3	19980502	1342	1456	1342	X1/3b	S15 W15	1.00	2000*	1044	1:14
4	20000217	1852	2006	1852	M2/1B	S25 W16	0.66	700	550	1:14
5	20000217	2025	2130	2035	M1/2N	S29 E07	1.17	550	~	1:06
6	20000404	1525	1632	1541	M1/2F	N16 W66	1.00	2000	984	1:07
7	20000606	1523	1554	1523	X2/3B	N20 E13	1.50	1189	908	0:31
8	20000714	1020	1054	1024	X6/3B	N22 W07	1.50	1800*	1775	0:34
9	20010120	1842	1931	1847	M1/SF	S07 E40	0.67	700	673	0:50
10	20010120	2114	2154	2120	M8/2B	S07 E46	1.00	1300	1576	0:40
11	20010128	1600	1554	1600	M1.5/?	S04 W59	1.00	1000**	795	-0:06

* velocity Vs is heuristically based on Vcme, not from metric II.

~ CME merged with the preceding CME as implied by "..part of preceeding CME was visible above S-pole from as early as 2006 UT" (Simon Plunkett, private communication, 2000).

****** Vs estimated from WIND/WAVES (kilometric II measurements).

$\mathbf{T_{cme}-T_{II}}$ time between the metric type II onset and the first CME observation.

$\mathbf{V_{cme}}$ velocity of the CME (private communication, from http:://lasco-www.nrl.navy.mil/cmelist.html); start time of the CME (column 4) is from real-time reports.

Column 1: Sequential event numbers. Column 2: Year, month and day. Cols. 3-4: Dates and observed starting times (UT) of each related metric Type II and halo CME. Column 5: Corresponding times of peak soft X-ray flux. Column 6: X-ray and optical flare classifications. Column 7: Solar disk locations. Column 8: The proxy piston-driving time (tau) of the shock as it moves at the Type II speed. Column 9: Velocities of the Type II radio bursts.
Column 10: Velocities of their related CMEs. Column 11: Metric Type II start minus CME start.

Table 2: Observed Interplanetary Shocks and the corresponding arrival predictions of 3 Numerical Models

1	2	3	4	5	6	7	8	9	10	11	12	13	14	15	16	17	18	19	20
Event	**IP Shock**							**STOA**		**ISPM**		**HAF-V2**		**DTs**	**DTi**	**DTh**	**Contingency**		
No.	Date		**S/c**	**Vtr**	**Vsh**	**Vsh/Vtr**	**TTd**	**TTs**	**Ma**	**TTi**	**SSI**	**TTh**	**SSI**	**pred.-obs.**			**Table-info**		
	YYMMDD	**UT**		(km/s)	(km/s)		(h)	(h)		(h)		(h)		(h)	(h)	(h)	**S**	**I**	**H-v2**
1	19970515	0115	W	612.7	467	0.76	68	46	7	30	1.3	37	0.13	-22	-39	-31	h	m	m
2	19971106	2218	W	651	495	0.76	64	52	4.8	40	0.9	41	0.01	-12	-24	-23	h	h	h
3	19980504	0225	A	1126	780	0.69	37	38	7.8	25	1.4	24	0.30	1	-12	-13	h	h	h
4	20000220	2047	A	563	487	0.86	74	75	1.5	81	0.5	63	0.30	1	7	-11	h	h	h
5	"	"	"	579	"	0.84	72	77	1.3	86	0.6	62	0.30	in	in	in	cn	cn	cn
6	20000406	1603	A	850	756	0.89	49	46	5.6	45	0.6	42	-0.13	-3	-4	-6.6	h	h	h
7	20000608	0841	A	1016	864	0.85	41	49	4.3	38	1	33	0.20	8	-4	-8.3	h	h	h
8	20000715	1417	A	1488	1150	0.77	28	29	7.9	25	1.4	28	0.35	1	-3	0	h	h	h
9	20010123	1007	A	661	660	1.00	63	89	1.4	mhd	-0	48	0.07	in	mhd	in	cn	cn	cn
10	"	"	"	683	"	0.97	61	62	3.7	51	0.6	46	0.07	1	-10	-15	h	h	h
11	20010131	0722	A	661	470	0.71	64	66	2.3	mhd	-0	71	-0.04	3	m	8	h	m	h

TTd Transit time from Sun to Earth
Vtr Transit velocity = 1AU / TTd,
$\mathbf{V_{sh}}$ Local shock velocity at 1AU (values for Events 1-3, 7,8 from D.B.: the rest were estimated by Z.S. assuming radial shocks.)
The shaded boxes are used to group the events closely spaced in time (#4,5 and #9,10) whose interplanetary shocks are expected to interact. See discussion in text. 'In' denotes interaction; 'mhd' decay to an mhd wave.
" standard symbol for "same as above"

Column 1: Event number as per Table 1. Cols. 2-4: Date and time of arrival of interplanetary shocks at WIND (W) and at ACE (A). Cols. 5-7: "Sun to L1" transit velocity (Vtr); estimate of the in situ shock speed (Vsh) and the ratio of these values. Column 8: The actual shock transit time data (TTd). Cols.9-10: The predicted transit times for STOA (TTs) and the modeled magneto-acoustic Mach number (Ma). Cols. 11-12: The predicted transit times for ISPM (TTi) and the modeled Shock Strength Index (SSI). Cols. 13-14: The predicted HAFv.2 transit times (TTh) and their corresponding Shock Searching Indices (SSI). Cols. 15-17: The arrival time errors (predicted minus the observed values) for each of the three models. Cols. 18-20: Elements of a statistical contingency table for the data set represented by hits (h); misses (m) and correct nuls)cn_